Multi-Variety Transcriptomic Analysis Identifies Oxalate and L-Ascorbate Oxidation as Key Pathways Driving High Oxalate Levels in Sour-Type Star Fruit

Ganhui Mo
Guangxi Subtropical Crops Research Institute
Yangfan Zhu
Guangxi Subtropical Crops Research Institute
Rasheed Usman
Guangxi Subtropical Crops Research Institute
Qinyu Lu
Guangxi Subtropical Crops Research Institute
Kaikai Meng
Guangxi Subtropical Crops Research Institute
Xiaohua Dai
Guangxi Subtropical Crops Research Institute
Shimiao Chen
Guangxi Subtropical Crops Research Institute
Haojun Chen
Guangxi Subtropical Crops Research Institute
Jingli Ou
Guangxi Subtropical Crops Research Institute
Ying Liu
groveno@163.com

Guangxi Subtropical Crops Research Institute

Research Article

Keywords: star fruit, oxalate metabolism, transcriptomics, L-ascorbate, oxalate oxidase

Posted Date: November 13th, 2025

DOI: https://doi.org/10.21203/rs.3.rs-7844594/v1

Additional Declarations: No competing interests reported.

Version of Record: A version of this preprint was published at Tropical Plant Biology on February 6th, 2026. See the published version at https://doi.org/10.1007/s12042-026-09458-z.

Abstract

Averrhoa carambola L. (family Oxalidaceae), known as star fruit, is a berry species found in tropical and subtropical regions, recognized for its unique crisp texture, high juiciness, and refreshing, slightly tangy flavor profile. *A. carambola* is known for its relatively high total oxalate content (fresh weight: 200–1840 mg/100 g), and excessive consumption is linked to toxicity, particularly in individuals with chronic kidney disease or other renal disorders. Therefore, understanding the mechanisms behind oxalate accumulation is crucial for developing effective strategies to manage oxalate levels in *A. carambola*. To our knowledge, this represents the first comprehensive transcriptomic investigation conducted across distinct fruit types of *A. carambola*. Results demonstrated that the downregulation of genes associated with oxalate oxidation contributes to the elevated oxalate content observed in sour-type *A. carambola* fruits. In addition, L-ascorbate concentration exhibits a positive correlation with oxalate levels across different varieties. These findings establish a foundational work for formulating rational and targeted strategies to regulate oxalate content in *A. carambola*, encompassing genetic improvement, optimized harvest timing, and carefully designed post-harvest management practices.

1. Introduction

Averrhoa carambola L. (Oxalidaceae), commonly known as star fruit, is a tropical to subtropical berry distinguished by its crisp texture, juiciness, and refreshing flavor(Ramadan et al. 2020). As a globally popular fruit, it is used in various culinary applications, including fresh consumption, beverages(Liu and Zhang 2006), salads, and cooked dishes(Nowak et al. 2023). Nutritionally, star fruit is valued for its antioxidant, hypoglycemic, hypotensive, hypocholesterolemic, and anti-inflammatory properties(Lakmal et al. 2021). However, star fruit contains relatively high levels of total oxalate (fresh weight: 200–1840 mg/100 g)(Pongener et al. 2022; Wilson et al. 1982; Zhong et al. 2009), and excessive intake has been associated with toxicity, particularly in individuals with chronic kidney disease(Signaté et al. 2009). Driven by the notion that reducing oxalate content could enhance the quality and safety of star fruit, agronomists are dedicated to developing superior varieties with lower oxalate levels while preserving their original flavor(Fan et al. 2020). Thus, A deeper understanding of the mechanisms underlying oxalate accumulation is thus critical for regulating oxalate levels in star fruit(Abduh et al. 2023). In model plants, research has elucidated key pathways of oxalate degradation and identified major metabolic precursors(Ermer et al. 2023), showing that oxalate homeostasis is governed by a complex gene network(Li et al. 2022b). In contrast, the molecular mechanisms controlling oxalate accumulation in star fruit remain poorly understood, and the genetic determinants of its oxalate content are largely unknown. Furthermore, since most prior studies have concentrated on herbaceous species, examining star fruit offers a unique opportunity to enhance the understanding of oxalate regulation in woody plants and broaden the current knowledge of oxalate metabolism.

Oxalate, the simplest dicarboxylic acid, is characterized by strong acidity (pKa_1 = 1.25; pKa_2 = 4.27), reducibility, and chelating capacity(Ermer et al. 2023). It is considered an anti-nutrient that interferes with mineral absorption and promotes calcium oxalate crystal formation, contributing to kidney-related

disorders(Rosenstock et al. 2022). Oxalate is widely distributed across plant species, with contents ranging from 3% to 80% of dry weight, and is particularly abundant in families such as Chenopodiaceae, Portulacaceae, Amaranthaceae, and Oxalidaceae(Nakata 2003). Within Oxalidaceae, certain varieties of *A. carambola* accumulate markedly higher oxalate levels than most common fruits(A. Al-Wahsh et al. 2012), with concentrations comparable to those found in spinach(Kawazu et al. 2003). Vegetal oxalates are generally classified as soluble or insoluble. Soluble forms include ammonium, sodium, and potassium oxalates, whereas insoluble forms primarily consist of calcium oxalate, magnesium oxalate, and heavy metal salts such as iron oxalate(Salgado et al. 2023). In food science, soluble oxalates in fruits and vegetables are generally regarded as harmful, whereas insoluble oxalates are considered less problematic because they are poorly absorbed across the intestinal epithelium and thus unlikely to enter systemic circulation or affect renal health(Zayed et al. 2025).

Oxalate inside star fruit quantified by HPLC following either acid extraction or neutral aqueous extraction showed no significant difference, indicating that estimates of the soluble–insoluble partition are minimally influenced by the extraction method under these conditions(Hönow and Hesse 2002). Zhong et al. further reported that the soluble fraction constitutes approximately 50–90% of total oxalate, and soluble oxalate levels are significantly higher in sour cultivars than in sweet cultivars(Zhong et al. 2009). Thus, the relatively high proportion of soluble oxalate in star fruit is strongly linked to the risk of kidney injury associated with excessive consumption.

Within a single crop, tissue oxalate levels vary substantially with genotype (cultivars), developmental stage, organ type, environmental conditions, and fertilization regime(Kaju et al. 2023). In star fruit, cultivars are broadly classified as sour or sweet based on distinct sugar–acid balances. Additionally, the organic acids composition in star fruit also shifts markedly during fruit ripening(Xu et al. 2024). In tart-type cultivars like ‘Golden Star’, oxalate makes up a significant portion of the organic acid pool when the fruit reaches commercial maturity. As the fruit progresses to the full-yellow stage, there is a decrease in tartaric acid content and lower titratable acidity(Babu et al. 2006). Oxalate distribution differs among plant organs as well, with leaves typically showing the highest accumulation(Li et al. 2022b). Consistent with this pattern, *A. carambola* leaf oxalate levels are nearly 1.5-fold greater than those of fruit on a dry-weight–equivalent basis (leaves: 5.92 g/100 g DW; fruit: 160–295 mg/100 g FW, equivalent to 3–4 g/100 g DW when normalized)(Sá et al. 2019). A similar pattern has been reported in kiwifruit (*Actinidia chinensis*), where the mesocarp also stores less oxalate(Rassam and Laing 2005).

In higher plants, oxalate biosynthesis primarily occurs through three pathways: (i) the glycolate–glyoxylate route associated with photorespiration, where glycolate is oxidized to glyoxylate by glycolate oxidase and subsequently to oxalate; (ii) the isocitrate (glyoxylate-cycle) route, in which isocitrate lyase generates glyoxylate; and (iii) the L-ascorbate route, in which oxalate is derived from the hydrolysis or oxidation of oxalyl-L-threonate, a downstream metabolite of dehydroascorbic acid(Cai et al. 2018). Additionally, a fourth pathway involving oxaloacetate acetyl-hydrolase (OXAC) has been proposed, primarily described in fungi(Liang et al. 2015); however, genetic evidence for this route in plants remains limited, with current knowledge largely restricted to beet and spinach(Rana et al. 2022). Plants also

biomineralize calcium oxalate (CaOx) crystals within specialized cells (idioblasts), producing morphotypes such as prismatic and druse that are distributed across tissues and taxa. Engineered *Arabidopsis* systems confirm the genetic sufficiency for crystal formation and highlight developmental regulation of this process(Cuéllar-Cruz et al. 2020). In *Averrhoa* spp., leaf studies are consistent with these morphotypes, but the crystal types and spatial distribution in fruit tissues remain unresolved, underscoring the need for targeted anatomical investigation(Lawrie et al. 2023). Oxalate catabolism proceeds through two major plant pathways. The oxidative route involves oxalate oxidase (OXO), typically a germin/germin-like protein activity that is widespread in cereals but less frequent, though present, in dicots(Li et al. 2022b). The CoA-dependent route relies on oxalyl-CoA synthetase (AAE3/OCS) and oxalyl-CoA decarboxylase (OXC) and contributes to CaOx crystal homeostasis as well as stress adaptation, including aluminum tolerance(Foster et al. 2016).

With respect to mining of genetic factors involved in oxalate metabolism regulation, the lack of uniformity in genetic backgrounds often impedes intraspecific transcriptome differential analysis from reliably identifying hotspot genes with potential biological significance related to the target phenotype. This difficulty arises from the challenge of attributing such identifications to physiological and biochemical properties. Furthermore, in transcriptomic studies, heterogeneous genetic backgrounds can introduce significant transcriptional noise, which obscures the identification of core genes that play essential functional roles. It is established that oxalate content in plants is a complex trait governed by multiple genetic loci. genomic-based methods for gene discovery such as conventional quantitative trait locus (QTL) mapping and modern genome-wide association studies (GWAS), require large populations exhibiting substantial genetic diversity to achieve sufficient statistical power.

To address these limitations, this study employs a multi-variety transcriptomic approach to systematically characterize the regulatory network of oxalate metabolism in star fruit. The research focuses on elucidating key metabolic pathways implicated in oxalate regulation at the transcriptional level, with the goal of identifying critical functional enzymes under tight gene-expression control. This work provides a foundation for unraveling the mechanisms of oxalate accumulation in star fruit and helps to fill a conceptual gap in the understanding of oxalate metabolism in this species. To our knowledge, this represents the first comprehensive transcriptomic comparison across varied types of *A. carambola*. We anticipate that this expression profiling will advance understanding of oxalate origin and metabolic flux in this species.

2. Materials and methods

2.1 Fruit material, sampling and oxalate content determination

A total of ten well-characterized *A. carambola* varieties (germplasm source) were selected. Fruits at the yellow-ripe (YR) stage (from April, 2024 to August, 2024) in triplicate (biological replicates) were harvested from the Star Fruit Germplasm Bank of the Guangxi Subtropical Crop Research Institute in

Nanning city, Guangxi Zhuang Autonomous Region, China (108°22' 55"E, 22°50' 49"N). To validate the key genes associated with oxalate oxidation and L-ascorbate oxidation metabolism pathways identified via WGCNA, 18 individuals of two varieties (nY6 = 8, nY5 = 10) were collected at the yellow-ripe stage from the Star Fruit Germplasm Bank of the Guangxi Subtropical Crop Research Institute. For RNA extraction and transcriptomic sequencing, pulp or core tissue (~ 1 cm^3 per piece) was sampled and frozen immediately in liquid nitrogen, and stored at -80°C. The remaining tissues were used for oxalate and ascorbate content determination.

The total oxalate content was measured using the hot extraction method described by Al-Wahsh et al(A. Al-Wahsh et al. 2012), combined with High-Performance Liquid Chromatography (HPLC)(Wilson et al. 1982). Briefly, fruit ribs and both ends were removed, and the remaining tissue without seeds was cut into pieces and homogenized. A 0.1 g aliquot of the homogenate was transferred to a 1.5 mL centrifuge tube, mixed with 0.9 mL of 2 N HCl, and incubated at 80°C for 30 min. The mixture was then centrifuged at 12,000 × g for 5 min. The supernatant was diluted 10-fold with distilled deionized water, filtered, and loaded into sample vials for HPLC analysis. HPLC detection was performed on a Waters e2695 system (Waters Corporation, USA) using a 7.8 mm × 300 mm Aminex HPX-87H column (Bio-Rad). The mobile phase consisted of 4 mM H_2SO_4, with a flow rate of 0.6 mL/min. Oxalate was detected at 210 nm (retention time: 6.5 min) using a UV detector. Anhydrous oxalate (75688-50g, Merck, Germany) was used as the standard for quantification.

2.2 RNA extraction, and transcriptomic sequencing

RNA extraction and transcriptome sequencing were conducted by VeryGenome Technology Co., Ltd. (Guangzhou, China). Total RNA was isolated using the HiPure HP Plant RNA Mini Kit (R4165-02, Magen, China) according to the manufacturer's instructions. RNA purity, concentration, and integrity were evaluated with a NanoPhotometer® (IMPLEN, CA, USA), Qubit® 3.0 Fluorometer (Life Technologies, CA, USA), and Agilent 2100 Bioanalyzer with the RNA Nano 6000 Assay Kit (Agilent Technologies, CA, USA), respectively. High-quality RNA was enriched for mRNA using oligo(dT)-conjugated magnetic beads, fragmented, and reverse-transcribed into first-strand cDNA with random hexamer primers. Second-strand cDNA was synthesized, and sequencing libraries were prepared by PCR amplification of the double-stranded cDNA. Sequencing was performed on the Illumina HiSeq platform, generating 150 bp paired-end reads. Raw data were processed and assembled, and unigenes were annotated using Blast2GO (https://www.blast2go.com/). Principal component analysis (PCA) was conducted with the "FactoMineR" package(Le et al. 2008) in R, and results were visualized using R package "factoextra".

2.3 Bioinformatics analysis

Weighted gene co-expression network analysis (WGCNA) was performed using the "WGCNA" R package(Langfelder and Horvath 2008). Transcriptomic data were primarily filtered to remove genes with a median absolute deviation (MAD) ≤ 10 and then variance-stabilized with the "varianceStabilizingTransformation" function in DESeq2(Love et al. 2014). The soft-thresholding power was set to 14, and modules were merged using a dissimilarity threshold of 0.25. To identify transcription

factors (TFs) within the “lightgreen” module, the gene list was analyzed using iTAK(Zheng et al. 2016) (http://itak.feilab.net/cgi-bin/itak/index.cgi). For TF binding site prediction, 2,000 bp upstream sequences of the coding DNA sequence (CDS) at *AcOXO19* locus were submitted to the Binding Site Prediction module in PlantRegMap (https://plantregmap.gao-lab.org/)(Tian et al. 2020). Gene set enrichment analysis(Subramanian et al. 2005) was performed and visualized using R package “clusterProfiler” and “GseaVis” respectively. The customized terms include five proposed oxalate metabolism pathways, i.e., glycolate oxidation, isocitrate lysis, L-ascorbate oxidation, oxalate acetylation and oxalate oxidation. GO and KEGG enrichment analysis were performed drawing on comprehensive bioinformatics analysis platform “KEYIYUN” (https://researcheasy.cn/).

2.4 Determination of L-ascorbate content

L-ascorbate content was determined using 2,6-Dichlorophenolindophenol titration method described by Tarrago-Trani et al(Tarrago-Trani et al. 2012). with some modification. Briefly, 200 μL of the fruit puree was weighed from homogenization and made up to a final volume of 2 mL with 2% oxalic acid solution, followed by agitation for 5 min to extract the L-ascorbate. Subsequently, 1 mL mixture was filtered and mixed with another 9 mL 2% oxalic acid solution for titration using 2,6-Dichlorophenolindophenol standard solution (0.1 g/L). Each sample was analyzed in triplicate. Titer of 2,6-Dichlorophenolindophenol standard solution was determined using L-ascorbate standard solution (0.1 g/L)

2.5 Quantitative reverse transcription PCR (qRT-PCR) verification of key genes

RNA was extracted from star fruit homogenate using FastPure Universal Plant Total RNA Isolation Kit (RC411-01, Vazyme, China) and subsequently subjected to reverse transcription using HiScript IV 1st Strand cDNA Synthesis Kit (+ gDNA wiper) (R412-01, Vazyme, China) according to manufacturers’ instructions after quantification and qualification via NanoDrop ONE instrument (ThermoFisher, the USA). Relative transcript levels were quantified by qRT-PCR, qPCR reactions (technical triplicates) were run using ChamQ Universal SYBR qPCR Master Mix (Q711-02, Vazyme, China), and relative expression was calculated by the $2^{-\Delta Ct}$ approach with GAPDH as the internal control. Sequences of primer pairs used were documented in Table.S1.

2.6 Statistical analysis and figure generation

t test for statistical significance, one-way ANOVA for multiple comparisons and Pearson’s correlation analyses were performed using GraphPad Prism 9.5.0; Figures were produced using R package “tidyverse” and GraphPad Prism 9.5.0.

3. Results

3.1 Determination of fruit total oxalate content (FW, mg/100 g) in ten *A.carambola* varieties

Ten *A.carambola* varieties with distinct sour or sweet tastes were selected and sampled at the yellow-ripe stage of fruit. Their total oxalate content of each variety represented by FW (mg/100 g) was quantified via hot extraction method integrated with HPLC. The quantification of oxalate content in ten carambola varieties showed significant differences in accumulation levels. Y6 had the highest total oxalate content in the fruit pulp, reaching 1752.0 ± 337.0 mg per 100 g of fresh weight, surpassing all other tested varieties. Y7 also exhibited a markedly elevated oxalate content at 1092.0 ± 211.9 mg per 100 g, followed by Y23 at 703.3 ± 148.2 mg per 100 g. Together, these three varieties (Y6, Y7, and Y23) formed distinct groups characterized by high oxalate accumulation. In contrast, the other seven varieties, Y11, Y8, Y20, Y3, Y22, Y24, and Y5, had relatively low oxalate levels, ranging from 162.2 to 229.2 mg per 100 g of fresh weight. These findings indicate that oxalate accumulation in carambola fruit pulp is highly genotype-dependent, with Y6 and Y7 representing high-oxalate phenotypes (Fig. 1).

a, b, c and d represent statistically significant differences from one another (adjusted $p \leq 0.05$ via ordinary one-way ANOVA).

3.2 Transcriptomic Profiling of ten carambola fruits and identification of documented genes involved in oxalate metabolism

A total of thirty transcriptome datasets were acquired, with comprehensive quality control metrics summarized in Table 1. Among the ten representative transcriptomes analyzed, the mean clean read count reached 47,638,730 M, accompanied by an average Q30 score of 99.42% and GC content of 44.35% (Table 1). Extended quality parameters are archived in Supplementary Table S2.

Table.1 Varietal information and quality control metrics of transcriptome data

Variety	AQ_reads_mean (M)	AQ_Q30R (%)	AQ_GC (%)
Y7	49299051	99.58 ± 0.34	44.23 ± 0.16
Y20	45303773	99.66 ± 0.02	44.30 ± 0.12
Y6	52229522	99.65 ± 0.02	44.03 ± 0.18
Y5	48588337	99.64 ± 0.04	44.31 ± 0.16
Y22	48674543	99.66 ± 0.04	44.50 ± 0.66
Y23	56736987	99.61 ± 0.26	44.19 ± 0.64
Y11	51452003	99.65 ± 0.05	44.32 ± 0.14
Y8	49657961	99.66 ± 0.06	44.27 ± 0.28
Y3	47920669	99.65 ± 0.01	44.22 ± 0.20
Y24	40729813	98.75 ± 0.03	44.78 ± 0.20
Average	47638730	99.42	44.35%

PCA of normalized gene expression counts demonstrated distinct varietal clustering patterns along the first two principal dimensions (Dim 1 vs Dim 2). Notably, varieties Y6, Y7, Y8, Y23, and Y24 formed a discrete cluster, whereas Y3, Y5, Y20, and Y22 that characterized by relatively lower oxalate concentrations, exhibited convergent spatial distribution (Fig. 2). This dimensional separation suggests transcriptomic divergence corresponding to oxalate accumulation phenotypes.

To investigate the transcriptional expression of previously reported oxalate metabolism–related genes in carambola fruit, we identified fifty-one unique unigene transcripts in the carambola transcriptome based on sequence homology (Table.S3). According to established oxalate metabolic pathways, fifty-one genes were classified into five groups: three oxalate biosynthetic pathways, namely glycolate oxidation, isocitrate cleavage, and L-ascorbate oxidation, two oxalate catabolic pathways, including oxalate oxidation and oxalyl-CoA acetylation. In the glycolate oxidation group, four glycolate oxidases (*AcGLOs*) and two phosphoglycolate phosphatases (*AcPGPs*) were identified. The isocitrate cleavage group comprised seven unigenes linked to the glyoxylate cycle, including malate dehydrogenase (*AcMDH*), citrate synthase (*AcCS*), aconitase, and isocitrate lyase (*AcICL*), among others. The L-ascorbate oxidation group contained twelve unigenes related to the L-ascorbate metabolic pathway, with most of the key enzymes for L-ascorbate anabolism present, suggesting a well-developed biosynthetic system in *A. carambola*; however, genes encoding the enzyme responsible for oxidative degradation of dehydroascorbate (DHA) to oxalate were not detected. In the oxalate oxidation group, twenty-two germin-like proteins (GLPs) were annotated as oxalate oxidases (*OXOs*), highlighting that oxalate oxidase represents a relatively large protein family in *A. carambola*. Finally, the oxalate acetylation group included four homologous genes, consisting of two oxalyl-CoA synthases (*AcAAE3-I* and *AcAAE3-II*), one oxalyl-CoA decarboxylase (*AcOXC*), and one formate dehydrogenase (*AcFDH*).

3.3 Weighted gene co-expression network analysis (WGCNA) of carambola fruit transcriptome data

A total of 24,532 unigenes were documented in the *A. carambola* reference transcriptome. For WGCNA analysis, 14,010 unigenes were selected based on a median absolute deviation (MAD) > 10. The samples exhibited clear clustering patterns corresponding to their respective varieties (Fig. S1). For gene co-expression network construction, a soft-thresholding power of 14 was selected based on network topology analysis (Fig. S2), and modules were merged at a height cutoff of 0.25 (Fig. S3), yielding sixteen distinct modules. Among these, four modules showed significant correlations with total oxalate content, with absolute gene significance (GS) values exceeding 0.6. Ranked by correlation strength, these included: “lightgreen” (GS = 0.84, *p* = 4e-09), “grey60”(G = 0.76, *p* = 1e-06), “darkgrey”（GS = 0.62, *p* = 2e-04）and “orange” （GS = -0.6, *p* = 4e-04）(Fig. 3A). Notably, genes within the "lightgreen" module demonstrated a strong positive correlation between GS and module membership (Fig.S4, r = 0.69, *p* = 4.8e-173).

Under the dual criteria of *p*.GS.FW_oxalate ≤ 0.05 and |GS.FW_oxalate| >0.6, WGCNA identified 1,854 significantly correlated genes, comprising 989 positively correlated and 865 negatively correlated genes, their transcriptomic count data were displayed in Fig. 3B. Among these, seven previously reported oxalate metabolism-related genes were included: *AcVTC2-II* (GS = 0.92, *p* = 9.8e-13, module = “lightgreen”), *AcPGP1* (GS = 0.63, *p* = 1.8e-4, module = “lightgreen”), *AcVTC2-I* (GS = 0.629, *p* = 1.9e-4, module = “lightgreen”), *AcOXO19* (GS = -0.88, *p* = 2.2e-10, module = “lightgreen”), *AcGLO1*(GS = -0.79, *p* = 1.7e-7, module = “blue”), *AcOXO4* (GS = -0.78, *p* = 2.9e-7, module = “grey60”), *AcOXO13* (GS = -0.685, *p* = 2.96e-5, module = “grey60”)(Fig.3C).

a. Module trait relationships regarding total oxalate content of carambola fruits; b. Normalized count data heatmap of 1,854 significant correlated genes; c. Volcano plot of 14,010 genes regarding GS.FW_oxalate and *p*.GS.FW_oxalate.

3.4 GSEA, GO and KEGG enrichment of significantly correlated genes identified by WGCNA

To transcriptionally assess the contribution of previously reported oxalate metabolism pathways in regulating oxalate content across different carambola fruit varieties, we performed gene set enrichment analysis (GSEA) on five classified pathways. This analysis utilized a gene set with *p*.GS.FW_oxalate ≤ 0.05 (n = 6,029) derived from WGCNA, which included 14 of the 51 annotated genes described earlier. The GSEA results revealed that the L-ascorbate oxidation pathway was activated in varieties with relatively high oxalate content (NES = 1.480, *p* = 0.0704), while the oxalate oxidation pathway showed marked suppression (NES = -1.714, *p* = 0.021). The remaining three pathways exhibited suppression with comparatively low significance, suggesting their marginal role in oxalate content regulation (Fig. 4A)

Subsequently, we conducted GO and KEGG enrichment analyses on the gene set comprising 989 positively correlated genes (GS > 0.6, *p*.GS.FW_oxalate ≤ 0.05). GO enrichment results revealed that the top three terms with respect to biological process (BP) are (1) “organonitrogen compound metabolism process”, (2) “cellular localization” and (3) “protein transport” in order. Regarding cellular component (CC), the top three terms are (1) “protein-containing complex”, (2) “respiratory chain complex” and (3) “proteasome core complex, alpha-subunit complex”. Regarding molecule function (MF), (1) “threonine-type endopeptidase activity”, (2) “protein-macromolecule adaptor activity” and (3) “SNAP receptor activity” ranked in the top three. KEGG enrichment analysis identified the following top three enriched pathways: (1) “proteasome”, (2) “oxidative phosphorylation” and (3) “ubiquitin mediated proteolysis” (Fig. 4B). These findings suggest an underlying relationship between organonitrogen metabolism and oxalate content. We postulate that a plausible mechanism for this could be the transformation of elevated oxalate to formate through decarboxylation, which subsequently serves as a critical one-carbon source for nitrogen metabolism. Nevertheless, larger amount of oxalate does not incite significant upregulation of *AcAAE3* or *AcOXC* among varieties in our WGCNA, presumably because the predominance of other catabolic pathways, such as oxidation, appears to be more critical for oxalate homeostasis.

As to the gene set containing 865 negatively correlated genes (GS < -0.6, *p*.GS.FW_oxalate ≤ 0.05), GO enrichment results revealed that the top three terms with respect to BP are (1) “ncRNA metabolic process”, (2) “ncRNA processing”, (3) “rRNA metabolic process” in order. Notably, epigenetic-related terms including "macromolecule methylation" (ranked 7th) and "methylation" (ranked 10th) were prominently identified among the enriched terms. Regarding CC, the top three terms are (1) “plastid”, (2) “chloroplast” and (3) “nucleolus”. Regarding MF, (1) “ATP-dependent activity”, (2) “snoRNA binding” and (3) “helicase activity” ranked in the top three. KEGG enrichment analysis revealed that (1) “ribosome biogenesis in eukaryotes”, (2) “aminoacyl-tRNA biosynthesis” and (3) “pyrimidine metabolism” ranked in the top three terms (Fig. 4C). These findings point to an underlying epigenetic mechanism regulating oxalate content, implicating that a sharp increase is driven by the transcriptional downregulation of degradation effector genes, which include certain transcription factors and enzymes.

a. GSEA of five oxalate metabolism pathways; b. GO and KEGG enrichment of positively correlated gene set; c. GO and KEGG enrichment of negatively correlated gene set.

3.5 L-ascorbate and oxalate contents from two varieties (Y6 & Y5) display positive correlation

GSEA revealed a pronounced activation of the L-ascorbate oxidation pathway in sour-type carambola fruits characterized by higher oxalate content, suggesting a positive correlation between L-ascorbate and oxalate accumulation (Fig. 5A). To validate this finding, we performed correlation analysis using eighteen biological replicates from two varieties (Y5 & Y6), while simultaneously comparing the relative expression levels of WGCNA-identified key genes (*AcVTC2-II*, *AcPGP1*, *AcVTC2-I*, *AcOXO19*, *AcGLO1*, *AcOXO4*, and *AcOXO13*) between varieties through qRT-PCR.

Consistent with our hypothesis, the dominant high-oxalate variety Y6 demonstrated significantly elevated L-ascorbate levels (Pearson's r = 0.72, $p = 0.0007$; Fig. 6A). Transcriptional patterns of *AcVTC2-II* and *AcPGP1* (upregulated) as well as *AcOXO19* and *AcOXO13* (downregulated) corroborated the WGCNA predictions. However, two discrepancies emerged: (1) *AcGLO1* showed unexpected upregulation in Y6, contrary to WGCNA results, and (2) neither *AcVTC2-I* nor *AcOXO4* exhibited significant differential expression between varieties (Fig. 5B).

a. Correlation analysis of L-ascorbate and oxalate content; b. Relative expression level validation of key genes (*AcVTC2-II*, *AcPGP1*, *AcVTC2-I*, *AcOXO19*, *AcGLO1*, *AcOXO4* and *AcOXO13*) between two *A. carambola* varieties by qRT-PCR. **: $p \leq 0.01$; ***: $p \leq 0.001$

3.6 Identification of key transcription factors governing *AcOXO19* expression divergence across *A. carambola* varieties

The AcOXO protein family, as direct effectors of oxalate degradation, plays a pivotal role in modulating oxalate content in carambola fruit. Among these, AcOXO19 emerged as the most prominent oxalate oxidase candidate identified through our WGCNA analysis. To investigate the molecular mechanisms underlying *AcOXO19* downregulation in sour-type star fruit, we integrated transcription factor binding site prediction with correlation analysis of genes co-expressed within the "lightgreen" module. Results showed that binding sites for MYB family(Stracke et al. 2001) are rich in expression regulatory region upstream promoter of *AcOXO19*(Fig. 6A), annotated member of MYB family *AcMYB5* had a significantly positive correlation with *AcOXO19* (Pearson's r = 0.7918, $p = 1.88e-7$) (Fig. 6B). These findings collectively suggest AcMYB5 as a putative transcriptional regulator of AcOXO19 in star fruit.

a. Genome-wide characterization of transcription factor binding landscapes in the *AcOXO19* regulatory region across *A. carambola* varieties;b. Pearson’s correlation analysis (*AcMYB5* vs *AcOXO19*). prop_TFBS: proportion of Transcription factor binding sites.

4. Discussion

Star fruit (*A. carambola*) is classified as a berry-a type of fleshy fruit-sharing anatomical features with representative berries like grapes(Cerri and Reale 2020). Cross-sectional analysis reveals a thin, waxy peel (exocarp) and a thick, fleshy layer (mesocarp). Parenchyma cells of *A. carambola* pulp featured large vacuoles dedicated to water and nutrient storage. Star fruit juice is highly acidic (pH 1.9-2.0) and watery(Babu et al. 2006). We measured juice pH across varieties and found that sour-type fruits had significantly lower pH (and higher oxalate content) than sweet-type fruits (unpublished data). Given that fruit juice primarily derives from vacuolar fluid, we hypothesize that the vacuole serves as the main oxalate reservoir in star fruit. However, determining the dominant form of oxalate (soluble vs. insoluble) in the vacuole remains challenging. Existing methods for quantifying oxalate forms are inadequate for star fruit, as its inherently acidic juice may solubilize most oxalate compounds-including calcium

oxalate. In addition to vacuole, localization data for pertinent enzymes (AcOXO, AcAAE3, AcOXC, AcGLO) indicate potential oxalate pools in the apoplast, cytoplasm, and peroxisome. Despite this, the precise spatial distribution of oxalate at both tissue and subcellular levels in star fruit awaits characterization.

The oxalate content serves as a critical quality parameter for fresh-eating star fruit. In this study, we employed a multi-variety transcriptomic analysis strategy to systematically investigate the genetic determinants underlying oxalate accumulation at the transcriptional level. Our findings reveal that the oxalate catabolism pathway dependent on oxidation constitutes a key regulatory mechanism responsible for the substantial inter-varietal variation in oxalate content. Notably, the sour-type star fruit variety Y6 exhibited pronounced transcriptional suppression of key functional enzymes within this metabolic pathway. qRT-PCR validation demonstrated significantly lower expression levels of oxalate oxidase-encoding genes (*AcOXO19* and *AcOXO13*) in Y6 compared to the sweet variety Y5. Among the oxalate oxidase family members identified in our transcriptome data, *AcOXO19* emerged as the most abundantly expressed gene. Collectively, these results establish the pivotal role of oxalate oxidation pathways in governing the differential oxalate accumulation patterns observed among starfruit varieties. However, OXO expression showed no significant changes in leaves from different spinach varieties, and only a trend of downregulation was observed in roots of spinach cultivar characterized with higher oxalate content, contrast to low oxalate content spinach(Joshi et al. 2021). This inconsistency might be caused by divergences in tissue types and species. Given the debated biochemical function of oxalate oxidase, validation of AcOXO enzyme activity is essential to confirm its role in oxalate degradation. Regarding the regulatory mechanism underlying the down-regulated transcriptional expression of *AcOXO19* in sour type star fruit, we identified putative transcription factor binding hotspots within the gene's promoter upstream cis-regulatory elements through bioinformatics analysis. Integrating this with WGCNA-based co-expression module analysis, it’s implied that *AcMYB5* may participate in the transcriptional regulation of *AcOXO19*. In this study, *AcMYB5* exhibits a significant negative correlation with oxalate content (GS = -0.77, p = 7.53e-7), consistent with observations in spinach varieties where high oxalate content is associated with suppressed MYB expression in root tissues(Joshi et al. 2021). Based on these findings, we propose that expression of *AcMYB5* is inhibited in sour type star fruit and thereby *AcOXO19* expression is suppressed. Additionally, epigenetic factors may be also involved in regulation of *AcOXO19* expression, in that terms pertaining to methylation are observed in GO enrichment results of significant negative correlated gene set.

For the other catabolism pathway dependent on oxalate acetylation, previous studies in tomato reported that *AAE3*-knockout lines exhibited improved fruit quality (higher sugar-acid ratio and mineral content) with a slight increase in oxalate levels(Li et al. 2022a). However, in this study, despite the negative correlation observed between genes associated with the oxalate acetylation pathway and oxalate levels in star fruit, the degree of correlation was weak. Consequently, we conclude that the regulatory expression of oxalate acetylation-related genes across different *A. carambola* varieties has minimal impact on oxalate levels.

Regarding oxalate anabolism, WGCNA revealed that the L-ascorbate oxidation pathway significantly contributes to oxalate accumulation in high-oxalate, acidic varieties of star fruit. This observation was corroborated by a correlation analysis of oxalate and ascorbic acid levels conducted in two distinct varieties—Y6 (acidic) and Y5 (sweet). Specifically, qRT-PCR results demonstrated that the relative expression of *AcVTC2-II* was markedly higher in the acidic Y6 variety compared to the sweet Y5. These findings strongly indicate a tight metabolic link between ascorbic acid and oxalate in star fruit, suggesting that ascorbic acid serves as a major precursor for oxalate biosynthesis. It is noteworthy that in Rosa cells, the apoplast has been identified as the site for ascorbic acid degradation—a compartment that also facilitates oxalate oxidation. The precise mechanistic relationship between these pathways, however, requires further elucidation.

Glyoxylate serves as a key precursor for oxalate biosynthesis in various plant species(Richardson and Tolbert 1961). Despite discrepancies between transcriptomic data and qRT-PCR results, our analysis of two *A. carambola* varieties (Y6 & Y5) revealed coordinated upregulation of *AcPGP1* and *AcGLO1* in the high-oxalate variety, suggesting the glycolate oxidation pathway contributes positively to oxalate accumulation. However, enzymatic components of this pathway showed limited transcriptional activity (mean TPM range: 11.4–94.0; Table S3), indicating potential pathway constraints in star fruit. In contrast, the L-ascorbate oxidation pathway emerged as a significant contributor (mean TPM range: 0.7–1162.5; Table S3). Nevertheless, L-ascorbate concentrations in star fruit remained markedly lower than accumulated oxalate levels(Zhu et al. 2019), suggesting potential alternative mechanisms for oxalate collection. Besides, alternative pathways such as isocitrate cleavage showed minimal involvement in oxalate biosynthesis, as evidenced by the negligible expression of *AcICL* (extremely low mean TPM: 0.0076; Table S3). These raise the question that whether endogenous oxalate synthesis alone is sufficient to account for the high oxalate content in star fruit.

As a C3 plant, *A. carambola* undergoes active photorespiration, producing large amounts of glycolic acid. This process likely drives substantial oxalate generation and accumulation in *A. carambola* leaves. Correspondingly, leaf and petiole tissues (adjacent to the fruit) have been reported to contain significantly higher oxalate levels, implying an exogenous source of oxalate from outside the fruit. Collectively, we propose three potential sources of oxalate accumulation in star fruit, other potential sources, such as oxaloacetate (a substrate for OXAC), cannot be excluded.

Exogenous oxalate from leaves

Oxalate may be transported from leaves to the fruit via vascular bundles, alongside other nutrients. This is supported by evidence that the fruit core-acting as a water and nutrient transport hub-contains higher oxalate levels than the pulp(Zhong et al. 2011). The predominant apoplast/cell wall localization of oxalate oxidase enables effective degradation of extracellular oxalate. Consequently, downregulation of the oxalate oxidase-encoding gene in sour type star fruit promotes oxalate accumulation and heightened concentrations. This supports the inference that exogenous oxalate represents a significant component and primary source of total oxalate within star fruit tissues.

Endogenous glycolic acid from local photorespiration

Star fruit may partially undertake photosynthesis and photorespiration, particularly in the exocarp. To estimate glycolate content in yellow-mature fruit, we adapted an HPLC method from Huang et al(Huang et al. 2014), yielding a glycolate level of approximate 100 mg/100 g (FW)-exceeding L-ascorbate levels (unpublished data). This aligns with reports that the peel and ribs (sites of active photorespiration) contain more oxalate than the pulp(Zhong et al. 2011).

Endogenous L-ascorbate

Star fruit contains substantial L-ascorbate reserves, with numerous functional enzymes identified in its L-ascorbate oxidation pathway. While our findings suggest a potential metabolic contribution of ascorbic acid to oxalate biosynthesis, the exact magnitude of this pathway's involvement requires validation through targeted genetic manipulation and enzymatic activity assays.

5. Conclusion

In summary, we demonstrated that downregulation of oxalate oxidation-related genes contributes to higher oxalate content in sour-type star fruit, and L-ascorbate content is positive correlated to oxalate among different varieties. We propose that the primary source of oxalate may be leaves rather than the fruit itself, supporting the hypothesis of exogenous oxalate in star fruit. Additionally, we identified two parallel oxalate metabolic pathways-one localized to the extracellular compartment and the other to the cytoplasm-that are critical for regulating oxalate content in star fruit. These findings provide a foundation for developing rational strategies to control oxalate content in star fruit, spanning genetic breeding, harvest timing, and post-harvest treatments.

Abbreviations

A. carambola: *Averrhoa carambola*; **GLO**: glycolate oxidase; **ICL**: isocitrate lyase; **OXAC**: oxaloacetate acetyl-hydrolase; **OXO**: oxalate oxidase; **AAE3**: acyl-activating enzyme 3; **OXC**: oxalyl-CoA decarboxylase; **PCA**: principal component analysis; **PCR**: Polymerase chain reaction; **HPLC**: High-performance liquid chromatography; **DEG**: differentially expressed gene; **FC**: fold change; padj: adjusted p-value; **TF**: transcription factor; **CDS**: coding DNA sequences; **qRT-PCR**: Quantitative reverse transcription PCR; **FW**: fresh weight; **PGP**: phosphoglycolate phosphatase; **MDH**: malate dehydrogenase; **CS**: citrate synthase; **DHA**: dehydroascorbate; **GLP**: germin-like protein; **FDH**: formate dehydrogenase; **BP**: biological process; **CC**: cellular component. **MAD**: median absolute deviation; **WGCNA**: weighted gene co-expression network analysis; **GS**: gene significance**SBP**: SQUAMOSA promoter binding proteins; **NES**: Normalized Enrichment Score; **GSEA**: gene set enrichment analysis. **ANOVA**: Analysis of Variance. **TPM**: Transcripts Per Million.

Declarations

Author contributions

Ying Liu is responsible for the conceiving, designing the experiments and drafting the manuscript. **Usman Rasheed** is responsible for reviewing and English polishing of the manuscript. **Ganhui Mo, Yangfan Zhu** and **Xiaohua Dai** are responsible for the sampling and homogenization of star fruits, qRT-PCR validation experiment as well as determination of L-ascorbate content. **Qinyu Lu** and **Shimiao Chen** are responsible for the oxalate content determination via HPLC, including the preparation of samples before detect. **Kaikai Meng** is responsible for bioinformatics analysis. **Haojun Chen** is responsible for the assistance in agronomics of star fruit. **Jingli Ou** is responsible for supervision, conceptualization and methodology.

Conflict of interest

The authors declare that they have no known competing financial interests or personal relationships that could have appeared to influence the work reported in this paper.

Acknowledgements

This work was supported Guangxi Academy of Agricultural Sciences Technology Development Fund (GUINONGKE2024ZX02), Pioneer Team for Science and Technology in the Specialty Fruit Industry (GUINONGKEMENG202504-04) and Guangxi Natural Science Foundation (2021GXNSFBA196005). We appreciate for the providing samples of different *A. carambola* varieties from colleagues in the fruit research center, Guangxi subtropical crops research institute, as well as for their assistance in plant cultivation. We would also like to thank **Jianmei Zhong**, an excellent Bioinformatics analyst, for her technological support and recommendation pertaining to our differential transcriptomic analysis.

Data availability

Data will be made available on reasonable request.

References

1. Al-Wahsh A, Wu I, Liebman Y M (2012) A Comparison of Two Extraction Methods for Food Oxalate Assessment. J Food Res 1(2):233. https://doi.org/10.5539/jfr.v1n2p233
2. Abduh MS, Saghir SAM, Al Hroob AM, Bin-Ammar A, Al-Tarawni AH, Murugaiyah V, Mahmoud AM (2023) *Averrhoa carambola* leaves prevent dyslipidemia and oxidative stress in a rat model of poloxamer-407-induced acute hyperlipidemia. Front Pharmacol 14:1134812. https://doi.org/https://doi.org/10.3389/fphar.2023.1134812
3. Babu KN, Minoo D, Tushar KV, Ravindran PN (2006) Carambola. In *Handbook of Herbs and Spices* (pp. 257–269). https://doi.org/10.1533/9781845691717.3.257
4. Cai X, Ge C, Xu C, Wang X, Wang S, Wang Q (2018) Expression Analysis of Oxalate Metabolic Pathway Genes Reveals Oxalate Regulation Patterns in Spinach. Molecules 23(6):1286.

https://doi.org/10.3390/molecules23061286

5. Cerri M, Reale L (2020) Anatomical traits of the principal fruits: An overview Scientia Horticulturae. 270:109390. https://doi.org/10.1016/j.scienta.2020.109390
6. Cuéllar-Cruz M, Pérez KS, Mendoza ME, Moreno A (2020) Biocrystals in Plants: A Short Review on Biomineralization Processes and the Role of Phototropins into the Uptake of Calcium. Crystals 10(7):591. https://doi.org/10.3390/cryst10070591
7. Ermer T, Nazzal L, Tio MC, Waikar S, Aronson PS, Knauf F (2023) Oxalate homeostasis. Nat Rev Nephrol 19(2):123–138. https://doi.org/10.1038/s41581-022-00643-3
8. Fan YN, Sahu SK, Yang T, Mu WX, Wei JP, Cheng L, Yang JL, Mu RC, Liu J, Zhao JM, Zhao YX, Xu X, Liu X, Liu H (2020) Dissecting the genome of star fruit (*Averrhoa carambola* L). Hortic Res 7(1):94. https://doi.org/https://doi.org/10.1038/s41438-020-0306-4
9. Foster J, Luo B, Nakata PA (2016) An Oxalyl-CoA Dependent Pathway of Oxalate Catabolism Plays a Role in Regulating Calcium Oxalate Crystal Accumulation and Defending against Oxalate-Secreting Phytopathogens in *Medicago truncatula*. PLoS ONE 11(2):e0149850. https://doi.org/10.1371/journal.pone.0149850
10. Hönow R, Hesse A (2002) Comparison of extraction methods for the determination of soluble and total oxalate in foods by HPLC-enzyme-reactor. Food Chem 78(4):511–521. https://doi.org/10.1016/s0308-8146(02)00212-1
11. Huang T, Wang S, Liu X, Liu H, Wu Y, Luo X (2014) Rapid determination of eight organic acids in plant tissue by sequential extraction and high performance liquid chromatography. Chin J Chromatogr 32(12):1356–1361. https://doi.org/10.3724/SP.J.1123.2014.09016
12. Joshi V, Penalosa A, Joshi M, Rodriguez S (2021) Regulation of Oxalate Metabolism in Spinach Revealed by RNA-Seq-Based Transcriptomic Analysis. Int J Mol Sci 22(10):5294. https://doi.org/10.3390/ijms22105294
13. Kaju J, Leelarungrayub J, Natakankitkul S, Laskin JJ (2023) Sweet-type star fruit supplementation controls oxidative stress status and enhances the community walking capacity among elderly Thai. Bmc Complement Med Ther 23(1):446. https://doi.org/10.1186/s12906-023-04291-3
14. Kawazu Y, Okimura M, Ishii T, Yui S (2003) Varietal and seasonal differences in oxalate content of spinach. Sci Hort 97(3–4):203–210. https://doi.org/https://doi.org/10.1016/S0304-4238(02)00154-1
15. Lakmal K, Yasawardene P, Jayarajah U, Seneviratne SL (2021) Nutritional and medicinal properties of Star fruit (*Averrhoa carambola*): A review. Food Sci Nutr 9(3):1810–1823. https://doi.org/https://doi.org/10.1002/fsn3.2135
16. Lawrie NS, Cuetos NM, Sini F, Salam GA, Ding HY, Vancolen A, Nelson JM, Erkens RHJ, Perversi G (2023) Systematic review on raphide morphotype calcium oxalate crystals in angiosperms. Aob Plants 15(4):plad031. https://doi.org/10.1093/aobpla/plad031
17. Li P, He Q, Jin J, Liu Y, Wen Y, Zhao K, Mao G, Fan W, Yang J (2022) Tomato Oxalyl-CoA Synthetase Degrades Oxalate and Affects Fruit Quality. Front Plant Sci 13:951386.

https://doi.org/10.3389/fpls.2022.951386

18. Li P, Liu C, Luo Y, Shi H, Li Q, PinChu C, Li X, Yang J, Fan W (2022) Oxalate in Plants: Metabolism, Function, Regulation, and Application. J Agric Food Chem 70(51):16037–16049. https://doi.org/10.1021/acs.jafc.2c04787
19. Liang XF, Liberti D, Li MY, Kim YT, Hutchens A, Wilson R, Rollins JA (2015) Oxaloacetate acetylhydrolase gene mutants of *Sclerotinia sclerotiorum* do not accumulate oxalic acid, but do produce limited lesions on host plants. Mol Plant Pathol 16(6):559–571. https://doi.org/10.1111/mpp.12211
20. Liu G, Zhang J (2006) Research on carambola beverage. Food Sci Technol 12:117–119. https://doi.org/10.13684/j.cnki.spkj.2006.12.035
21. Nakata PA (2003) Advances in our understanding of calcium oxalate crystal formation and function in plants. Plant Sci 164(6):901–909. https://doi.org/10.1016/s0168-9452(03)00120-1
22. Nowak D, Goslinski M, Przygonski K, Wojtowicz E (2023) *Averrhoa carambola* L., *Cyphomandra betacea*, *Myrciaria dubia* as a Source of Bioactive Compounds of Antioxidant Properties. Foods 12(4):753. https://doi.org/https://doi.org/10.3390/foods12040753
23. Pongener M, Sarkar A, Humtsoe L (2022) Studies on Biodiversity and Physico-chemical Properties of Carambola (*Averrhoa Carambola* L.) in Nagaland. Int J Bio-resource Stress Manage 13(9):906–913. https://doi.org/https://ojs.pphouse.org/index.php/IJBSM/article/view/4296
24. Ramadan NS, Wessjohann LA, Mocan A, Vodnar DC, El-Sayed NH, El-Toumy SA, Mohamed DA, Aziz ZA, Ehrlich A, Farag MA (2020) Nutrient and Sensory Metabolites Profiling of *Averrhoa Carambola* L. (Star fruit) in the Context of Its Origin and Ripening Stage by GC/MS and Chemometric Analysis. Molecules 25(10):2423. https://doi.org/https://doi.org/10.3390/molecules25102423
25. Rana K, Yuan JH, Liao HM, Banga SS, Kumar R, Qian W, Ding YJ (2022) Host-induced gene silencing reveals the role of *Sclerotinia sclerotiorum* oxaloacetate acetylhydrolase gene in fungal oxalic acid accumulation and virulence. Microbiol Res 258:126981. https://doi.org/10.1016/j.micres.2022.126981
26. Rassam M, Laing W (2005) Variation in ascorbic acid and oxalate levels in the fruit of *Actinidia chinensis* tissues and genotypes. J Agric Food Chem 53(6):2322–2326. https://doi.org/10.1021/jf048197s
27. Richardson KE, Tolbert NE (1961) Oxidation of Glyoxylic Acid to Oxalic Acid by Glycolic Acid Oxidase. J Biol Chem 236(5):1280–1284. https://doi.org/10.1016/s0021-9258(18)64165-1
28. Rosenstock JL, Joab TMJ, DeVita MV, Yang YH, Sharma PD, Bijol V (2022) Oxalate nephropathy: a review. Clin Kidney J 15(2):194–204. https://doi.org/10.1093/ckj/sfab145
29. Sá RD, Vasconcelos AL, Santos AV, Padilha RJR, Alves LC, Soares LAL, Randau KP (2019) Anatomy, histochemistry and oxalic acid content of the leaflets of *Averrhoa bilimbi* and *Averrhoa carambola*. Revista Brasileira de Farmacognosia 29(1):11–16. https://doi.org/10.1016/j.bjp.2018.09.005
30. Salgado N, Silva MA, Figueira ME, Costa HS, Albuquerque TG (2023) Oxalate in Foods: Extraction Conditions, Analytical Methods, Occurrence, and Health Implications. Foods 12(17):3201.

https://doi.org/10.3390/foods12173201

31. Signaté A, Olindo S, Chausson N, Cassinoto C, Nana ME, Saint Vil M, Cabre P, Smadja D (2009) Star fruit (*Averrhoa carambola*) toxic encephalopathy. Rev Neurol 165(3):268–272. https://doi.org/10.1016/j.neurol.2008.06.011
32. Wagner CJ Jr, Bryan WL, Berry RE, Knight RJ Jr (1975) Carambola selection for commercial production. In Proceedings of the Florida State Horticultural Society (Vol. 88, pp. 466–468)
33. Wilson CW, Shaw PE, Knight RJ (1982) Analysis of oxalic acid in carambola (*Averrhoa carambola* L) and spinach by high-performance liquid-chromatography. J Agric Food Chem 30(6):1106–1108. https://doi.org/10.1021/jf00114a025
34. Xu X, Xu L, Yang Z, Chen L, Wang Y, Ren H, Zhang Z, El-Kassaby YA, Wu S (2024) Identification of key gene networks controlling organic acid and sugar metabolism during star fruit (*Averrhoa carambola*) development. BMC Plant Biol 24(1):943. https://doi.org/10.1186/s12870-024-05621-4
35. Zayed A, Adly GM, Farag MA (2025) Management Strategies for the Anti-nutrient Oxalic Acid in Foods: A Comprehensive Overview of Its Dietary Sources, Roles, Metabolism, and Processing. Food Bioprocess Technol 18(5):4280–4300. https://doi.org/10.1007/s11947-024-03726-0
36. Zhong Y, Jiang B, Jiang N, Liu Y, Liu C, Zeng F, Yi G (2009) Quality analysis and determination of oxalic acid content of different varieties of carambola. GUANGDONG AGRICULTURAL Sci 12:67–69. https://doi.org/10.16768/j.issn.1004-874x.2009.12.053
37. Zhong Y, Jiang N, Jiang B, Liu Y, Zheng J, Yi G (2011) Distribution and Change of the Oxalic Acid Content in Carambola Fruit. Chin J Trop Crops 32(01):83–85. https://doi.org/10.3969/j.issn.1000-2561.2011.01.017
38. Zhu YF, Rong T, Chen H, Zhou J, Chen Y, He J, Ning L, Gan W, Pan Z, Ou JL (2019) Analysis of sugar, acid and antioxidant contents in carambola fruit at ripening stage. South China Fruits 48(5):39–43. https://doi.org/10.13938/j.issn.1007-1431.20190328

Figures

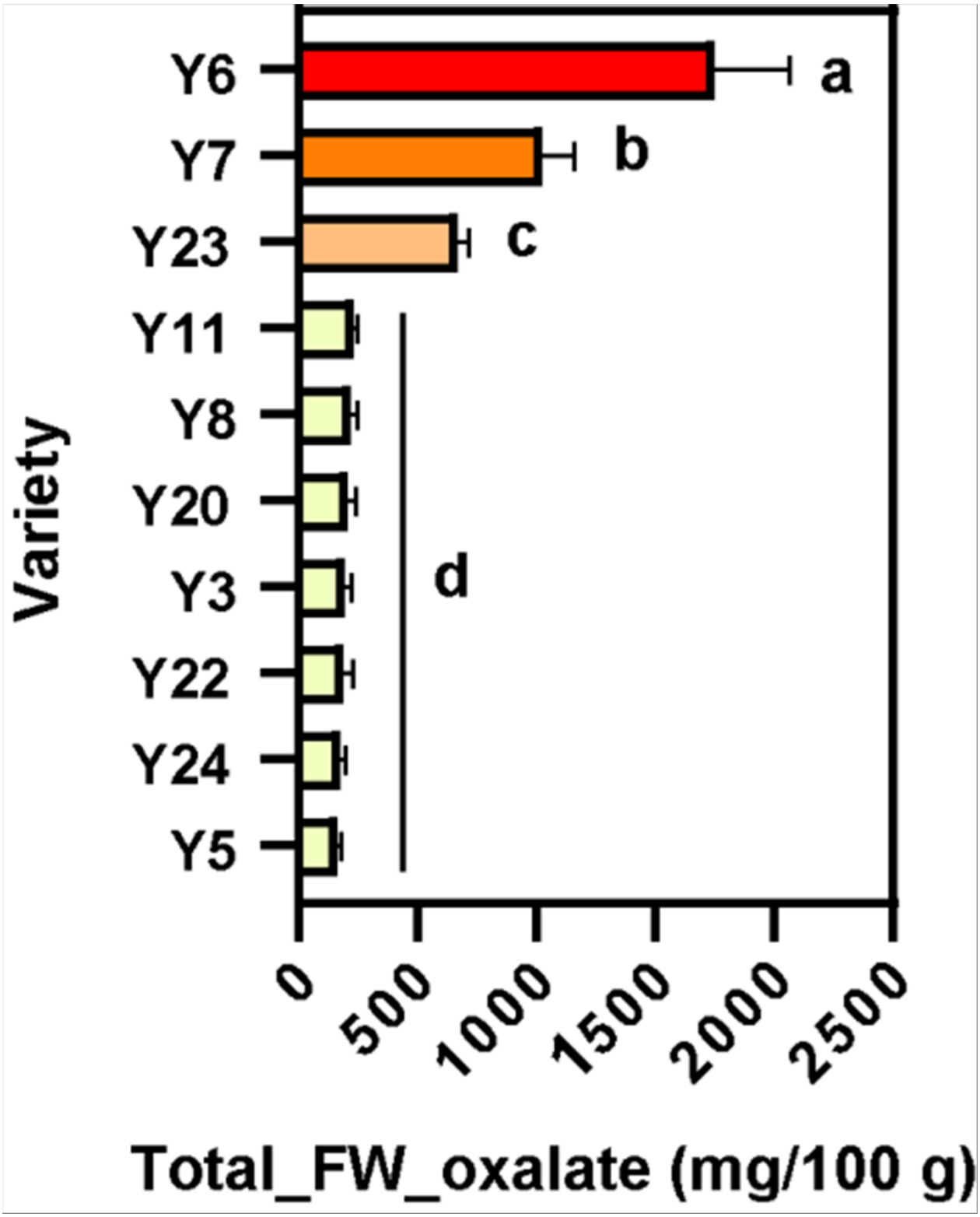

Figure 1

Total oxalate content of *A.carambola* fruits

a, b, c and d represent statistically significant differences from one another (adjusted $p \leq 0.05$ via ordinary one-way ANOVA).

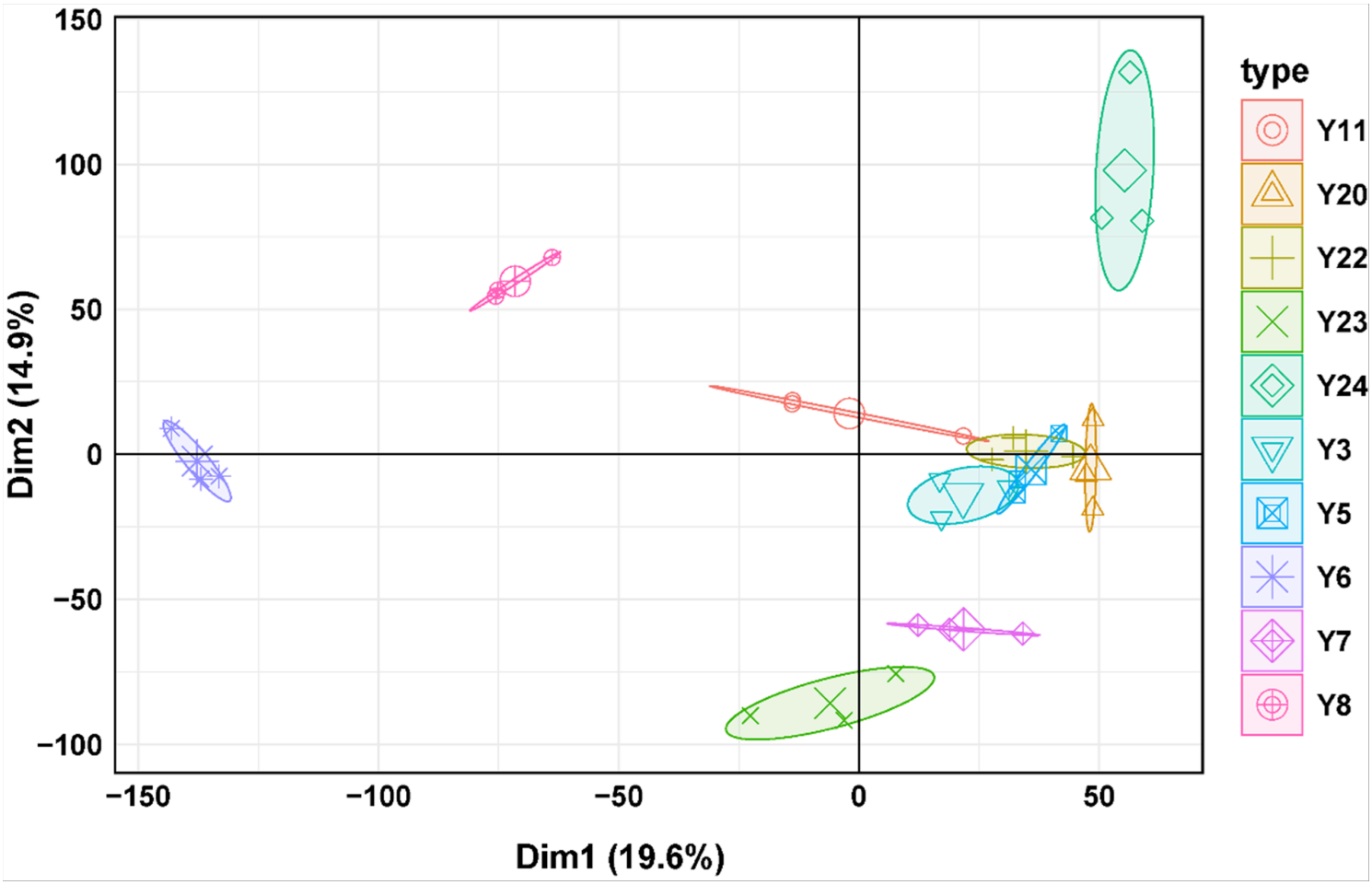

Figure 2

PCA of expression count data from ten carambola varieties

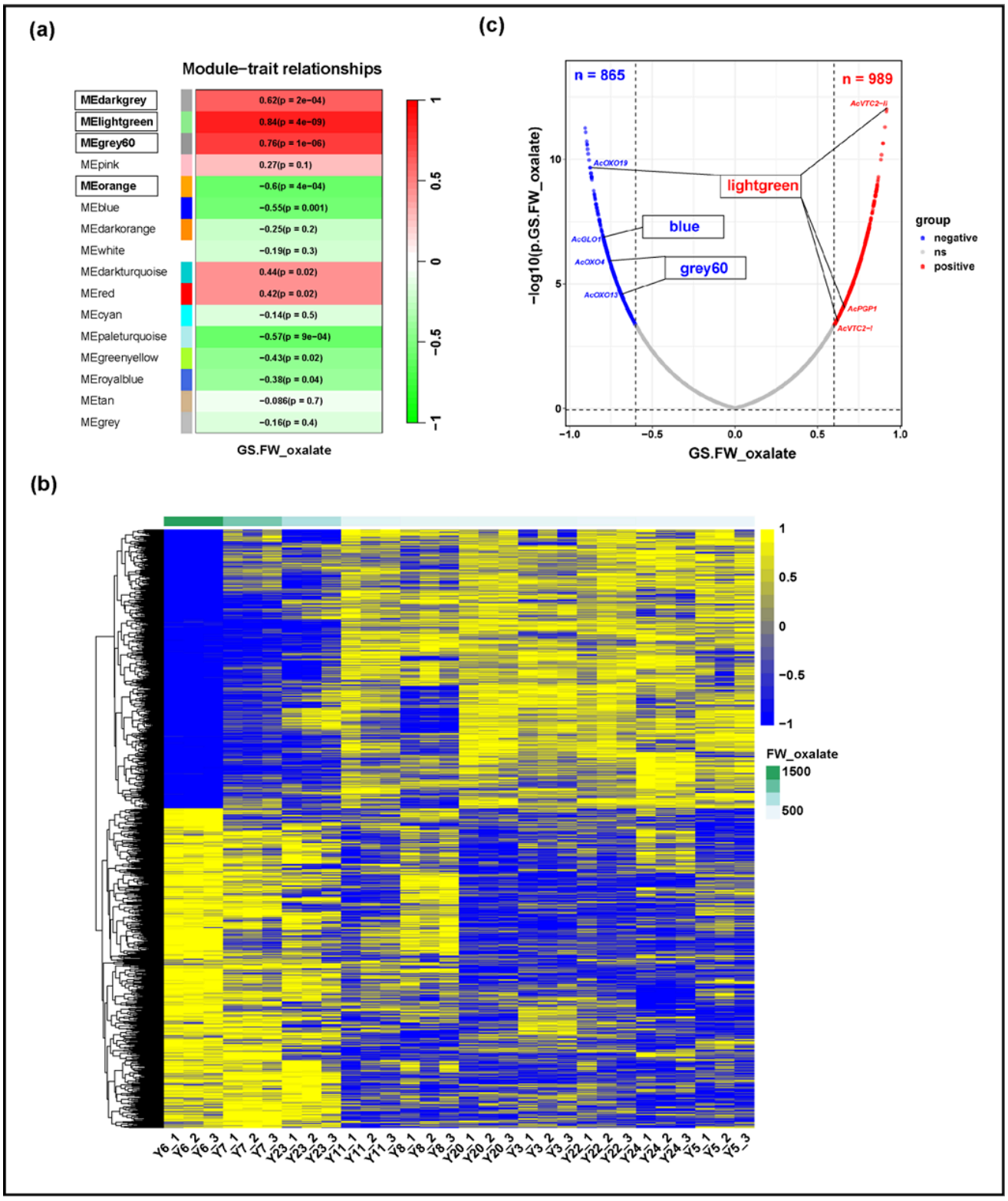

Figure 3

WGCNA results

a. Module trait relationships regarding total oxalate content of carambola fruits; b. Normalized count data heatmap of 1,854 significant correlated genes; c. Volcano plot of 14,010 genes regarding GS.FW_oxalate and *p*.GS.FW_oxalate.

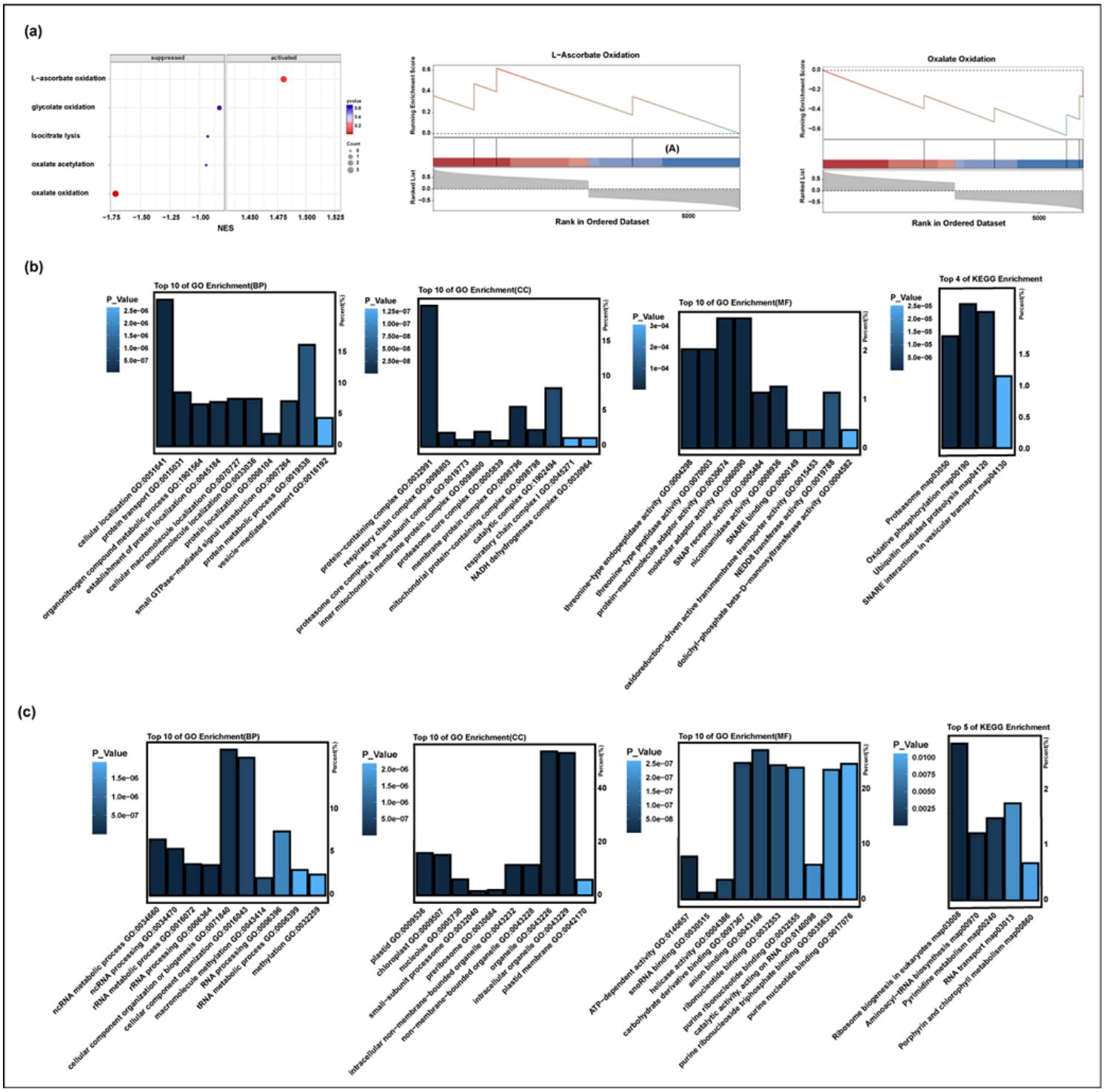

Figure 4

GSEA, GO and KEGG enrichment results

a. GSEA of five oxalate metabolism pathways; b. GO and KEGG enrichment of positively correlated gene set; c. GO and KEGG enrichment of negatively correlated gene set.

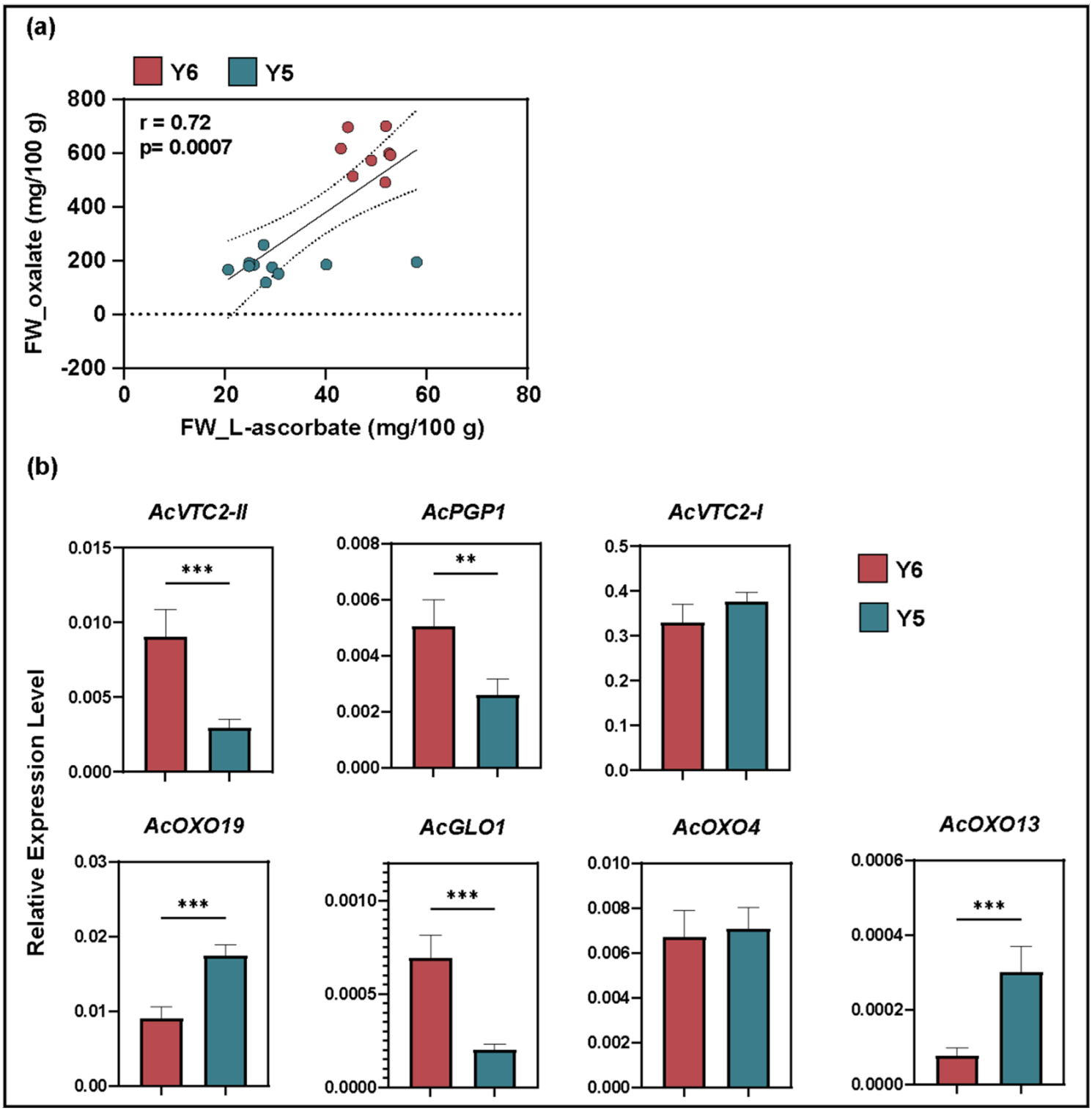

Figure 5

Investigating the metabolic relationship Between L-Ascorbate and Oxalate accumulation in *A. carambola* Fruits

a. Correlation analysis of L-ascorbate and oxalate content; b. Relative expression level validation of key genes (*AcVTC2-II*, *AcPGP1*, *AcVTC2-I*, *AcOXO19*, *AcGLO1*, *AcOXO4* and *AcOXO13*) between two *A. carambola*varieties by qRT-PCR. **: $p \leq 0.01$; ***: $p \leq 0.001$

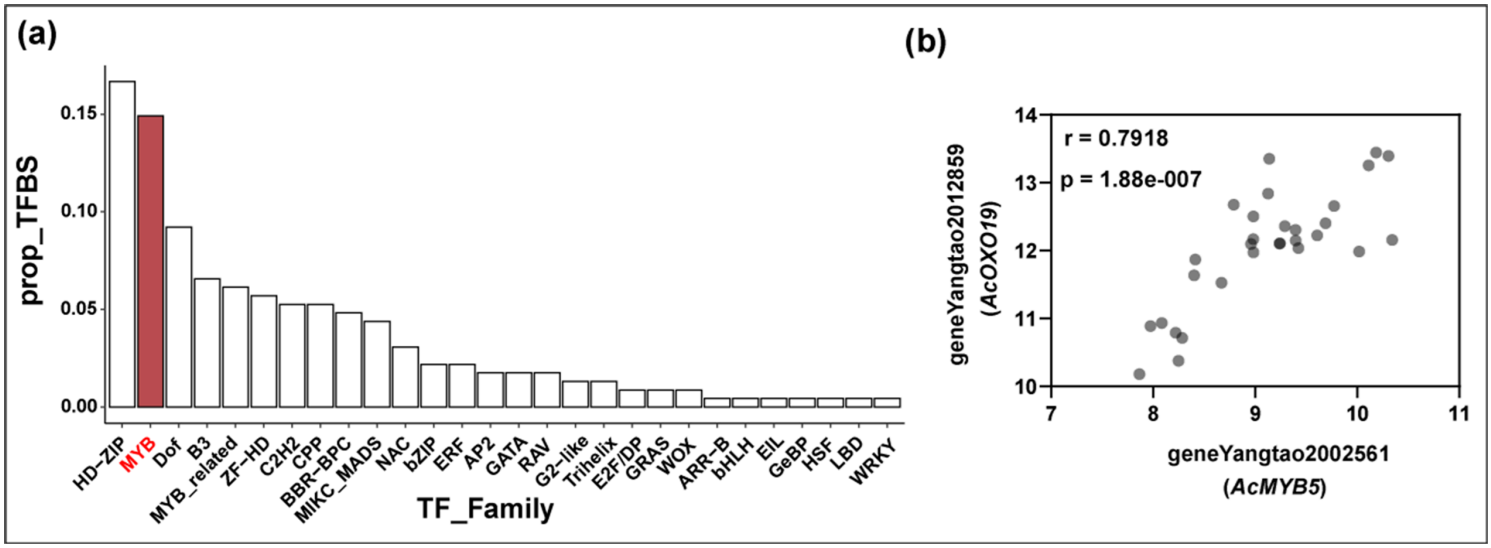

Figure 6

Exploration of potential transcription regulative factors of *AcOXO19*.

a. Genome-wide characterization of transcription factor binding landscapes in the *AcOXO19* regulatory region across *A. carambola* varieties b. Pearson's correlation analysis (*AcMYB5* vs *AcOXO19*). prop_TFBS: proportion of Transcription factor binding sites.

Supplementary Files

This is a list of supplementary files associated with this preprint. Click to download.

- Table.S1sequencesofprimerpairsforqRTPCR.xlsx
- Table.S2QCtranscriptomedata.xlsx
- Table.S3documentedoxalatemetabolismrelatedgenes.xlsx
- Figure.S1sampledendrogramandtraitheatmap.tif
- Figure.S2ScaleindependenceandMeanconnectivity.tif
- Figure.S3Clusteringofmoduleeigengenes.tif
- Figure.S4Modulemembershipvsgenesignificanceinlightgreen.tif